A Time-Domain Method for Numerical Noise Analysis of Oscillators

Makiko Okumura

R & D Center, Toshiba Corporation,
1, Komukai Toshiba-cho, Saiwai-ku,
Kawasaki 210, Japan
Tel: +81-44-549-2284
Fax: +81-44-520-1806
e-mail: *okumura@csl.rdc.toshiba.co.jp*

Hiroshi Tanimoto

R & D Center, Toshiba Corporation,
1, Komukai Toshiba-cho, Saiwai-ku,
Kawasaki 210, Japan
Tel: +81-44-549-2285
Fax: +81-44-520-1806
e-mail: *tanimoto@csl.rdc.toshiba.co.jp*

Abstract— A numerical noise analysis method for oscillators is proposed. Noise sources are usually small and can be considered as perturbations to a large amplitude oscillation. Transfer functions from each noise source to the oscillator output can be calculated by modeling the oscillator as a linear periodic time-varying circuit. The proposed method is a time domain method and can be applied to strongly nonlinear circuits. Thermal noise, shot noise and flicker noise are considered as noise sources. Error in the time domain method is also discussed.

I. Introduction

Estimation of noise is important in oscillator circuit design; however, it is difficult since an oscillator is a nonlinear circuit periodically changing its operating point. Simulation methods for phase noise of an oscillator are described in [1] [2]. However, the method using harmonic balance[1] is practical only for weakly nonlinear circuits, because it requires extremely large memory and computational time for highly nonlinear circuits. Reference [2] does not treat oscillators including flicker-noise sources. It is well known that flicker noise up-converted from the base band dominates around the oscillation frequency. A simulation including flicker noise is of prime practical importance for oscillator design. Our proposed method can simulate noise in strongly nonlinear circuits with flicker noise sources.

This paper is a natural extension of our previous work[3] to autonomous systems. In order to calculate the noise transfer functions, the oscillator is modeled as a linear periodic time-varying circuit, under the assumption that noise is small. A set of linear periodic time-varying discrete equivalent circuits is obtained during numerical integration for one period of the oscillation. Each equivalent circuit is evaluated at numerical integration time steps.

Analyses of oscillator noise[4][5][6] have been discussed using simple *R-L-C* resonator model. In reference [4], oscillator noise was represented by two terms: one is a linear component for diode's capacitor and the other is the first order nonlinear component. In reference [5], high order components were analyzed using high order nonlinear capacitor. All these nonlinear components were considered to be related to up-converted components of the oscillator noise. However, actually, some nonlinear components are up-converted from baseband and some nonlinear components are down-converted from high frequency bands. In this paper, up-converted noise components and down-converted noise components are related to the periodic time-varying transfer function which is calculable.

The algorithm has been implemented in a SPICE based circuit simulator SPREAD[3]. Noise sources considered were thermal noise, shot noise and flicker noise. Flicker noise was approximated by a stationary colored noise. In Section II, the noise analysis method is described. Two examples are shown in Section III. One is a Wien bridge oscillator and the other is a multivibrator. It is found that our time domain method is effective from these simulation results. However, on the other hand, the result is different from an estimate by using a conventional simple model. It is found that this discrepancy was caused by "losses" in numerical integration. In Section IV, this loss is considered in numerical integration algorithms. This paper is summarized in Section V.

II. Noise analysis method

A. State equation for autonomous system

Consider a nonlinear autonomous system:

$$f(y(t), \dot{y}(t)) = 0 \tag{1}$$

where $\dot{y}(t)$ denotes the time derivative of $y(t)$. It assumes that system (1) has a stable periodic solution $y_{st}(t)$ with period T:

$$y_{st}(t+T) = y_{st}(t) \quad \text{for all } t$$

ASP-DAC '97
0-89791-851-7/$5.00 ©1997 IEEE

The steady-state periodic solution can be computed using the shooting method [7][8], or simply using transient analysis.

Consider the perturbation to the system (1) around the periodic steady-state solution $y_{st}(t)$:

$$f(y_{st}(t), \dot{y}_{st}(t)) + \frac{\partial f}{\partial y}\delta y(t) + \frac{\partial f}{\partial \dot{y}}\delta \dot{y}(t) = 0$$

The above equation can be rewritten as

$$g(t)x(t) + c(t)\dot{x}(t) = 0, \tag{2}$$

where

$$x(t) \equiv \delta y(t), \ \dot{x}(t) \equiv \delta \dot{y}(t),$$
$$g(t) \equiv \frac{\partial f}{\partial y}, \quad c(t) \equiv \frac{\partial f}{\partial \dot{y}}.$$

Note that $g(t)$ and $c(t)$ are T-periodic, i.e., $g(t+T) = g(t)$ and $c(t+T) = c(t)$. System (2) is a linear periodic time-varying circuit.

B. Power spectrum of oscillator noise

The above system (2) can be represented by a periodic time-varying transfer function;$H(\Omega, t)$[9]. The transfer function is also T-periodic, its Fourier coefficients are obtained by

$$H_l(\Omega) = \frac{1}{T}\int_0^T H(\Omega, t)e^{-jl\omega_o t}dt, \tag{3}$$

where $\omega_o = 2\pi/T$. $H_l(\Omega)$ represents magnitude and phase for frequency translated output. $H_l(\Omega)$ can be interpreted as the transfer function with frequency translation for the output response with a frequency of $\Omega + l\omega_o$ when the input frequency is Ω.

Assuming stationary noise sources, output noise spectral density from the k-th noise source in the periodic time-varying circuit is given by[10]

$$S_k(\omega) = \sum_{l=-\infty}^{\infty} \left| H_l(\omega - l\omega_o) z_k \sqrt{s_k(\omega - l\omega_o)} \right|^2, \tag{4}$$

where $s(\cdot)$ indicates power spectral density of the k-th noise source. z_k is a vector which indicates noise source location. For example, when a noise source is connected to the q-th state, the q-th element of z_k is "1" and the remaining elements are "0". $H_l(\omega - l\omega_o)$ is a transfer function for output frequency ω when input frequency is $\omega - l\omega_o$.

Now, $H_0(\omega)$ is not involved with any frequency translation, that is, $H_0(\omega)$ is related to a linear component. For $l \neq 0$, $H_l(\omega - l\omega_o)$ are involved with frequency translation, that is, $H_l(\cdot)$ are related to nonlinear components. For example, $H_1(\omega - \omega_o)$ is related to an up-converted component, and $H_{-1}(\omega + \omega_o)$ is related to a down-converted component.

Assuming finite noise band, we consider a truncated version of (4):

$$S_k(\omega) = \sum_{l=-L}^{L} \left| H_l(\omega - l\omega_o) z_k \sqrt{s_k(\omega - l\omega_o)} \right|^2. \tag{5}$$

The power of each component is summed up until its contribution become negligible, or until the output noise converges.

The total rms noise of the oscillator is calculated by

$$N_{\rm rms}(\omega) = \sqrt{\sum_{k=1}^{M} S_k(\omega)}. \tag{6}$$

C. Calculation of noise transfer functions

Apply a unit complex sinusoidal signal at the k-th noise source to calculate the noise transfer function:

$$g(t)x(t) + c(t)\dot{x}(t) = z_k e^{j\Omega t} \tag{7}$$

For computing $H_l(\Omega)$ numerically, first divide the period T into p intervals.

$$T = \sum_{m=1}^{p} h_m, \quad \tau_m = \sum_{k=1}^{m} h_k, \quad \tau_p = T \quad , \tau_0 = 0.$$

Then, the integration of (3) can be replaced by a summation

$$H_l(\Omega) = \frac{1}{T}\sum_{m=1}^{p} H(\Omega, \tau_m) K_m^l \tag{8}$$

where $H(\Omega, \tau_m)$ is a time sampled version of $H(\Omega, t)$ at $t = \tau_m$, K_m^l is defined by

$$K_m^l \equiv \begin{cases} h_m & l = 0 \\ \dfrac{1 - e^{-j\omega_o h_m}}{jl\omega_o} e^{-jl\omega_o \tau_{m-1}} & l \neq 0. \end{cases}$$

Next, consider how to compute $H(\Omega, \tau_m)$ in (8). Since g and c are periodic, evaluating (7) at $t = nT + \tau_m$, we have

$$g_m x(nT + \tau_m) + c_m \dot{x}(nT + \tau_m) = z_k e^{j\Omega(nT + \tau_m)}. \tag{9}$$

The differential equation (9) is numerically solved by applying the backward Euler method to give

$$(g_m + \frac{c_m}{h_m})x(nT + \tau_m) - \frac{c_m}{h_m}x(nT + \tau_{m-1}) = z_k e^{j\Omega(nT + \tau_m)}. \tag{10}$$

The relationship between $H(\Omega, \tau_m)$ and $x(nT + \tau_m)$ can be written as

$$x(nT + \tau_m) = H(\Omega, \tau_m) z_k e^{j\Omega(nT + \tau_m)}. \tag{11}$$

Substituting (11) into (10) gives

$$\begin{bmatrix} J_1 & & & & C_1 \\ C_2 & J_2 & & & \\ & \cdot & \cdot & & \\ & & \cdot & \cdot & \\ & & & C_p & J_p \end{bmatrix} \cdot \begin{bmatrix} X_1 \\ X_2 \\ \cdot \\ \cdot \\ X_p \end{bmatrix} = \begin{bmatrix} z_k \\ z_k \\ \cdot \\ \cdot \\ z_k \end{bmatrix} \qquad (12)$$

where

$$X_m = X(\Omega, \tau_m) = H(\Omega, \tau_m) z_k,$$

$$J_m = g_m + \frac{c_m}{h_m}, \quad C_m = -e^{-j\Omega h_m} \frac{c_m}{h_m}.$$

The discretization step h_m is the numerical integration time step in the transient analysis for the periodic steady-state response.

The analysis flow is as follows:

Step 1. Compute a steady-state solution of oscillator.

Step 2. Store linear discrete equivalent circuits during numerical integration for one steady-state period.

Step 3. Compute noise transfer functions using equivalent circuits obtained in Step 2.

Step 4. Accumulate linear component and frequency sifted components(nonlinear components) using equation (8).

Step 5. Compute total noise using equation (6).

III. Simulation Results

Two examples are shown: one is a Wien bridge oscillator and the other is an emitter-coupled multivibrator. The periodic solution was calculated using the shooting method. The experimental program used the backward Euler method for numerical integration.

A. Wien bridge oscillator

The first example is shown in Fig. 1. The steady-steady solution is shown in Fig. 2. This circuit oscillated at 141.655 kHz. Noise sources considered were thermal noise of resistors, shot noise of diodes and bipolar transistors and flicker noise of diodes and transistors. Figure 3 shows the noise model of transistor. Flicker noise was approximated by a stationary colored noise. L value in equation (5) was 8. Figure 4 shows noise spectral density of total noise and a line spectrum of the steady-state oscillator output. The noise in this figure contains both amplitude noise and phase noise. This realizes a similar situation when the output is measured by a spectrum analyzer.

Figure 5 shows noise spectral density for some major noise sources. The horizontal axis is offset frequency, f_m, from the oscillation frequency. The noise spectral density near the oscillation frequency is flat in Fig.5. It is

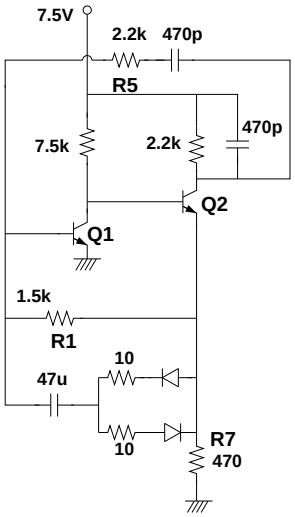

Fig. 1. Wien bridge oscillator

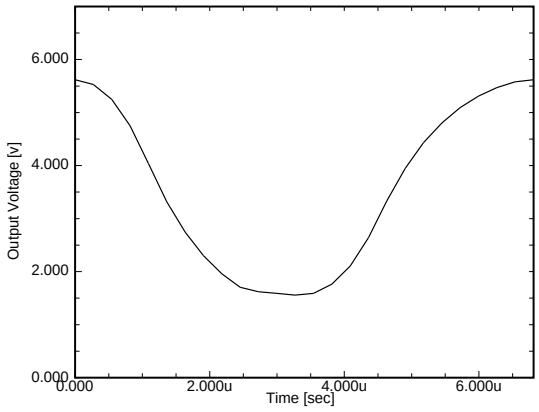

Fig. 2. Steady-state periodic solution of oscillator

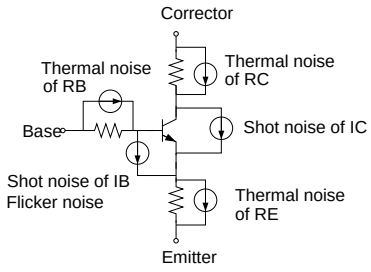

Fig. 3. Noise model of transistor

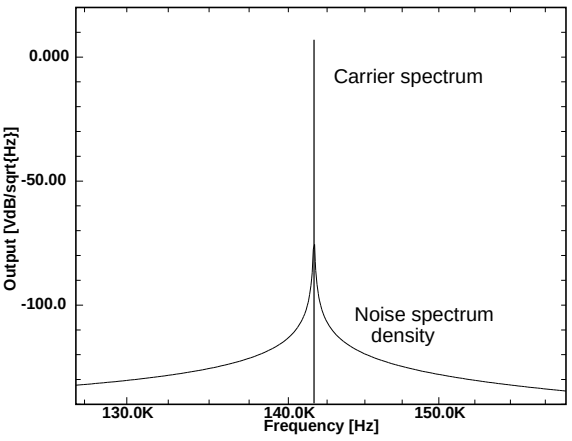

Fig. 4. Noise spectral density and carrier spectrum

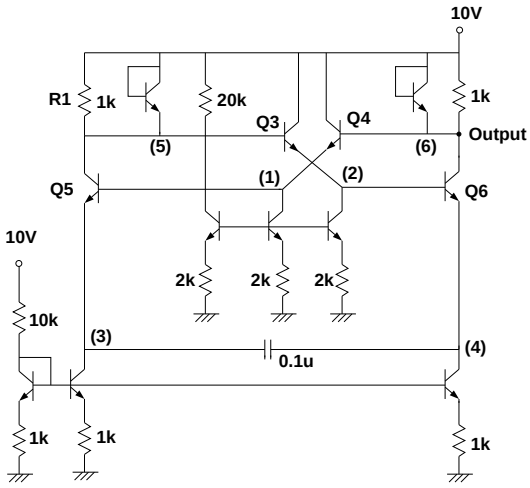

Fig. 6. Voltage controlled emitter-coupled multivibrator

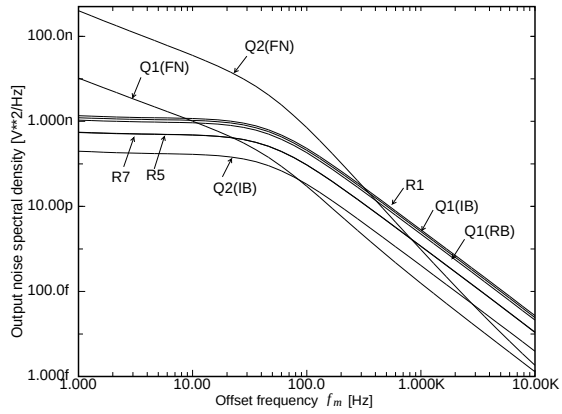

Fig. 5. Noise spectral density for major noise source

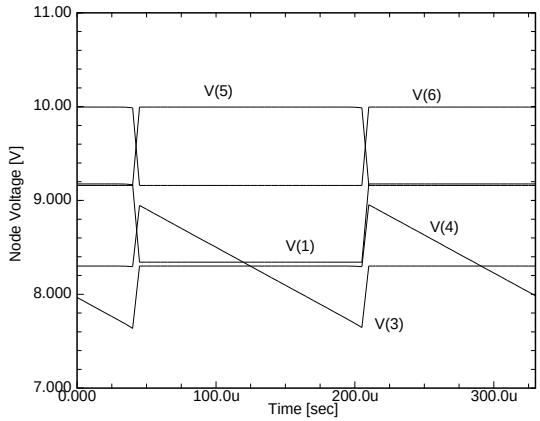

Fig. 7. Steady-state response of multivibrator

well known that noise spectral density for oscillator decreases with f_m at 9 dB/octave where $1/f$ effects predominate, and at 6 dB/octave where $1/f$ effects no longer predominate[11]. Our result is different from this. It is considered that the cause is an error in the numerical analysis. The error is discussed in Section IV.

B. Multivibrator

The second example is a voltage controlled emitter-coupled multivibrator shown in Fig. 6. This circuit cannot be simulated using the harmonic balance method because very high order Fourier components are needed. The steady-state responses of each node are shown in Fig. 7. Aliasing from wide frequency band should be considered for this example and L value in equation (5) was 31 while $L = 8$ for the linear Wien bridge oscillator. This clearly shows the frequency shifted components from high frequency bands are large for strongly nonlinear oscilla-

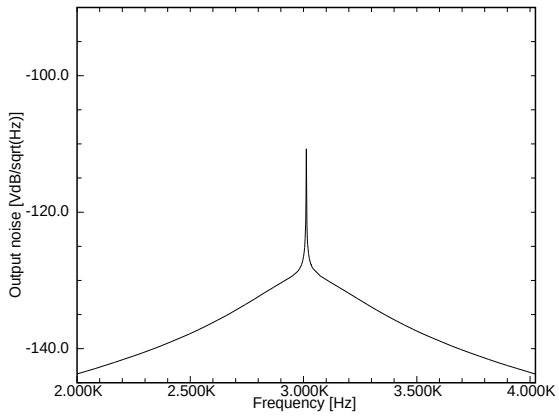

Fig. 8. Noise spectral density of multivibrator

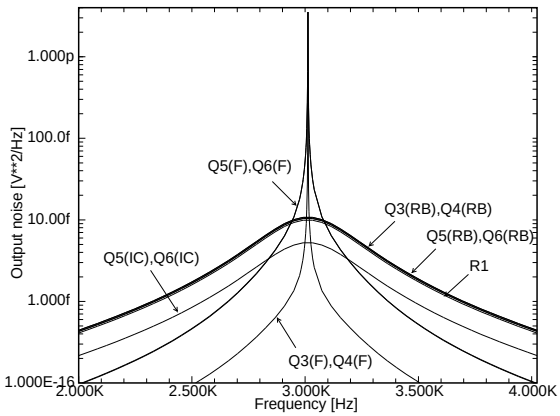

Fig. 9. Noise spectral density of dominant noise source

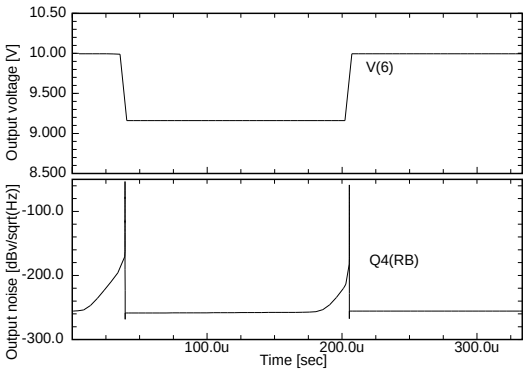

Fig. 10. Noise spectral density for the time domain and output voltage

tors. Again, thermal noise, shot noise and flicker noise are taken into account. The number of noise sources is 82. Total noise spectrum at the output is shown in Fig. 8. Noise spectral densities from several major sources are shown in Fig. 9. It was found that thermal noise of RB in transistor Q3, Q4, Q5, Q6 and of R1 and shot noise of Q6 and Q5 were important in this circuit. Flicker noise was dominant near the oscillation frequency. However, noise spectral density curves, with the exception of flicker noises, have flat tops, because Q value becomes finite due to the loss of the numerical integration. This will be discussed in Section IV.

Figure 10 shows $H(\Omega, \tau_m) \times \sqrt{4kTG}, m = 1, 2, \ldots, p$ in (8) for the thermal noise of RB in Q3 and output voltage for a single period. The output noise is large when transistors are active and switching. It is suggested that the average of these noises over one period decreases if transistors operate faster, as has been experienced by many designers. This kind of simulation becomes possible since our method is a time domain method.

IV. Discussion

The simulation results were different from the fact that noise spectral density decreases with f_m at 6 dB/octave where there is no flicker noise. It is believed that this is attributable to a lossy numerical integration method used for this particular implementation of the algorithm. Analysis of this phenomenon is discussed in this section.

The error in the transfer function calculation ϵ is defined by

$$\epsilon = \hat{H}(\Omega, \tau_m) - H(\Omega, \tau_m),$$

where $\hat{H}(\Omega, \tau_m)$ is an exact solution at time τ_m and $H(\Omega, \tau_m)$ is the numerical solution. From (11), we have

$$\hat{H}(\Omega, \tau_m) = \hat{x}(nT + \tau_m) e^{-j\Omega(nT+\tau_m)},$$

$$H(\Omega, \tau_m) = x(nT + \tau_m) e^{-j\Omega(nT+\tau_m)}.$$

Therefore,

$$\epsilon = \{\hat{x}(nT + \tau_m) - x(nT + \tau_m)\} e^{-j\Omega(nT+\tau_m)}. \quad (13)$$

From (13), the error magnitude for transfer function can be considered to be the same as the local truncation error[12] of the numerical integration algorithm, because $|e^{-j\Omega(nT+\tau_m)}| = 1$. In the frequency-domain approach[1], solutions for linear subnetworks are exact, while solutions by the time-domain approach cannot be exact even for the linear subnetwork.

Reference [3] describes the frequency warping effects for the backward Euler algorithm and the trapezoidal algorithm in conjunction with the time-domain approach. These algorithms are popular transformations between the s- and z-domain in the design of digital filters. A unit circle on z-plane maps by the following relations:

Backward Euler method:

$$s = \frac{1 - \cos \omega h}{h} + j \frac{\sin \omega h}{h} \quad (14)$$

Trapezoidal method:

$$s = j \frac{2}{h} \tan \frac{\omega h}{2}, \quad (15)$$

where $z = e^{j\omega h}$ and h is a uniform time step. It is found that backward Euler algorithm generates loss since (14) has a non-zero real part, while trapezoidal algorithm does not.

Reference[3] describes that the simulated Q value decreases relative to the actual Q value in the backward Euler algorithm. It is noted that the relative error caused by discretization tends to increase when high Q circuit is simulated. On the other hand, the relative error of the Q value in the trapezoidal algorithm is zero. An oscillator has an infinite Q value when the circuit is in a stable

oscillation. The equivalent circuit needs to compensate for the losses introduced by the numerical integration to continue to oscillate.

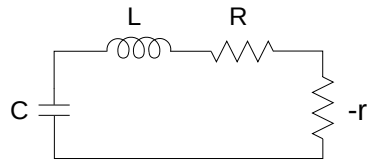

Fig. 11. Simple model for an oscillator with a resonator

Figure 11 shows a simple model of an oscillator with a resonator. The negative resistor stands for the gain of active elements. The positive resistor R is equal in magnitude to the negative resistor $-r$ in a stable oscillation. Then, the Q value is infinity. However, a magnitude of the negative resistor r in the equivalent circuit becomes larger than the positive resistor R, if the oscillation is maintained by using lossy numerical integration algorithm. This is because $R_C + R_L + R$ should be equal to r instead of $R = r$, where R_C and R_L are the losses generated during the numerical integration, to maintain oscillation.

For the second order Gear's algorithms, Laplace transform variable "s" is mapped by

Second order Gear's method:

$$s = \frac{1}{2h}\{3 - 4\cos(\omega h) + \cos(2\omega h)\} + j\frac{1}{2h}\{4\sin(\omega h) - \sin(2\omega h)\}. \quad (16)$$

Equation (16) also has a non-zero real part. The second order Gear's algorithm is also lossy. Therefore, oscillators should be simulated by using lossless numerical integration algorithms. To this end, the trapezoidal algorithm is the best for oscillator simulation. If the backward Euler method is used, a sufficiently small time step h is needed. However, it leads to an increase in computational time and requires a large memory.

V. Summary and Conclusion

A numerical noise analysis method for oscillators was presented. The linear periodic time-varying discrete equivalent circuits were obtained during numerical integration for one period of oscillation. Simulation results of a Wien bridge oscillator and a multivibrator were shown. Noise sources considered were thermal noise, shot noise and flicker noise. Flicker noises up-converted from the base band were dominant near the oscillation frequency. This method can simulate noise in strongly nonlinear circuits such as multivibrators and can observe noise spectrum evolution in time domain. However, it is found that implementation of the algorithm using lossy numerical integration cannot accurately simulate oscillator noise. We are now doing further study in order to implement the algorithm using the trapezoidal method and verify the results by comparing them with measured noise data.

References

[1] A. Howard, "Simulate oscillator phase noise," in *Microwaves & RF*, Vol.32, No.11, pp.64–70, November 1993.

[2] A. Demir and A. L. Sangiovanni-Vincenteli, "Simulation and modeling of phase noise in open-loop oscillators," *IEEE CICC*, 1996.

[3] M. Okumura, T. Sugawara and H. Tanimoto, "An efficient small signal frequency analysis method for nonlinear circuits with two frequency excitations," *IEEE Trans.* CAD, Vol.9, No.3, pp.225-235, March 1990.

[4] Allen A. Sweet, "A general analysis of noise in Gunn oscillators," *Proceedings of the IEEE*, pp.999-1000, August 1972.

[5] T.Ohira, " Higher-order analysis on phase noise generation in varactor-tuned oscillators–baseband noise upconversion in GaAs MESFET oscillators–," *IEICE Trans. Electron*, Vol.E76-C, No.12, pp.1851–1854, Dec. 1993.

[6] K. Kurokawa, "Noise in synchronized oscillators," *IEEE Trans. Microwave Theory and Techniques*, Vol.MTT-16, No.4, pp.234-240, April 1968.

[7] F.B.Grosz and T.N.Trick, "Some modifications to Newton's method for the determination of the steady-state response of nonlinear oscillatory circuits," *IEEE Trans. Comput.-Aided Des. Integrated Circuits Syst.*, Vol.CAD-1, No.3, pp.116–119, July 1982.

[8] M. Kakizaki and T. Sugawara, "A modified Newton method for the steady-state analysis," *IEEE Trans. CAD,* Vol. CAD-4, no. 4, pp. 662–667, Oct. 1985.

[9] L. A. Zadeh, "Frequency analysis of variable networks," *Proc. IRE*, Vol.32, pp.291–299, Mar. 1950.

[10] M.Okumura, H.Tanimoto, T.Itakura and T.Sugawara, "Numerical noise analysis for nonlinear circuits with a periodic large signal excitation including cyclostationary noise sources," *IEEE Trans. Circuits Syst., I: Fundamental Theory and Applications*, Vol.40, No.9, pp.581–590, Sept. 1993.

[11] D. B. Leeson, " A simple model of feedback oscillator noise spectrum," *Proceedings of the IEEE*, pp.329–330, Freb. 1966.

[12] L.O.Chua and P.M.Lin, *Computer-aided analysis of electronic circuits*, Prentice-Hall,Inc.,1975.